Insights into the Mechanism of the Catalytic Conversion of Glucose to Glycolaldehyde

[1]Rui Chen and [2]Xiaolei Zhao,
[1,2]College of Chemistry and Chemical Engineering, Henan Polytechnic University, Jiaozuo, Henan, China

Abstract—The catalytic conversion of glucose to glycolaldehyde is a promising method. However, the intricate details of this transformation mechanism remain unclear. In this study, Density Functional Theory calculations were employed using generalized gradient approximation under periodic boundary conditions to investigate the mechanism of glucose converting to glycolaldehyde on the $WO_3(020)$ surface. Four glucose adsorption configurations and their interactions with the surface were systematically examined. The potential conversion mechanisms were analyzed through energy barriers and reaction energies. Two pathways for the transformation of glucose into glycolaldehyde were proposed: one involving the further conversion of 1,2-ethenediol formed from glucose cleavage into glycolaldehyde, and the other where erythrose formed from glucose cleavage proceeds to glycolaldehyde. Comparative analysis reveals that the activation energy barrier (1.02 eV) for the conversion of erythrose formed from glucose degradation to glycolaldehyde is lower than the activation energy barrier (1.61 eV) for the conversion of 1,2-ethenediol formed from glucose degradation to glycolaldehyde. Hence, glycolaldehyde is more likely derived from the erythrose formed during glucose degradation.

Keywords—*Glucose; Glycolaldehyde; Catalytic Conversion; Reaction Mechanism; Wo₃;*

I. INTRODUCTION

In recent years, glycolic acid has attracted significant attention as a raw material for resin production. Glycolaldehyde serves as a precursor to glycolic acid, which is currently synthesized through various methods involving formaldehyde, propylene glycol, or ethylene glycol. Although traditional glycolaldehyde production techniques are valuable for quantitative manufacturing purposes, they involve the use of petrochemicals, catalysts, and microorganisms, necessitating significant waste management. As petroleum reserves decline and carbon dioxide emissions rise, research has turned towards cleaner, more sustainable alternative resources.[1-8]

Biomass stands out as the Earth's exclusive renewable carbon source, offering a promising foundation for sustainable fuel and chemical production.[9-14] Cellulose, the most prevalent biomass component, makes up 35 to 50% of lignocellulosic materials.[15] Its inedible nature sets it apart from starch, allowing for extensive use without endangering food supplies. Consequently, the catalytic conversion of cellulose into fuels and chemicals has gained increasing attention from the academic and industrial communities. However, the inherent resistance of cellulose presents a formidable challenge for its targeted depolymerization under gentle and eco-friendly conditions. The conventional use of inorganic acids for cellulose hydrolysis raises substantial environmental issues, whereas novel enzymatic degradation methods remain costly and inefficient.[16-18] Conversely, chemical catalysis pathways open up fresh avenues for the direct conversion of cellulose into chemicals, particularly by leveraging multifunctional catalysts to orchestrate cascading reactions leading to desired end products, thereby mitigating undesired side reactions stemming from unstable intermediates.[19-21]

Glucose, a repeating unit of cellulose, serves as a critical chemical intermediate in the production of various synthetic polymers within the petrochemical industry.[22] The conversion of glucose to glycolaldehyde through aldol condensation is a vital process for generating C2 products such as ethylene glycol,[23-25] ethanol,[26-28] and glycolic acid.[29-31] Zhang et al.[32] identified W-based compounds as highly active and selective catalysts for cellulose C-C cleavage to produce ethyl glycosides. Furthermore, the relatively high activation energy (140-150 kJ/mol) required for C-C cleavage enables the reaction to proceed more selectively at elevated temperatures (above 200°C).[33-36]

The comprehension and clarification of the reaction mechanism involved in the conversion of glucose to glycolaldehyde are crucial for the multi-step cascade reactions in cellulose transformation. Therefore, the WO3 catalyst was selected to investigate the reaction mechanism of glucose conversion to glycolaldehyde. For clarity, the entire work is divided into two parts. In the first part, the reaction mechanism involving the breaking of the C2-C3 bond in glucose to form glycolaldehyde is studied. In the second part, the reaction mechanism involving the cleavage of the C-C bond in the glucose C2-C3 cleavage product, erythrose, to form glycolaldehyde is investigated.
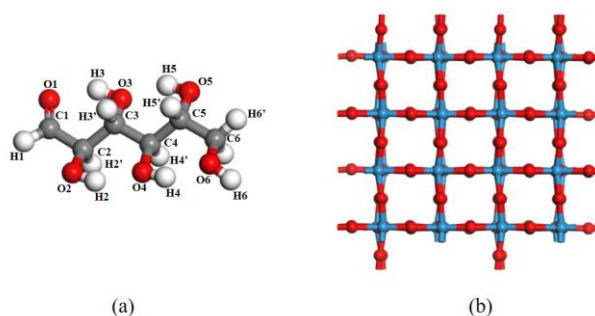
II. COMPUTATIONAL METHODS

Fig. 1. The optimized structures of glucose model molecule (a) and $WO_3(020)$ surface(b) (color code: blue–W, red–O, grey–C and white–H).

Periodic DFT slab calculations were performed using the Vienna ab initio simulation package (VASP)[37, 38]. Core and valence electrons were modeled with the projector augmented wave (PAW) method using a kinetic cutoff energy of 400 eV. The generalized gradient approximation (GGA) combined with the Perdew-Burke-Ernzerhof (PBE) functional describing the exchange-correlation functional was used in the calculations[39, 40]. Brillouin zone integration was performed with a $1×1×1$ Monkhorst−Pack (MP) k-mesh. The self-consistent field and force convergence criteria for structural optimization were set to $1 × 10^{-5}$ eV and 0.01 eV/Å, respectively. The $WO_3(020)$ surface, modeled as a P(2×2) supercell periodic slab with five layers, underwent energy minimization, allowing relaxation of adsorbates and atoms in

the upper two layers, while fixing atoms in the bottom three layers. A 15 Å vacuum layer separated surface slabs to prevent image interaction. Atom numbering for glucose molecules is referenced in Fig. 1(a), with the optimized WO₃(020) surface depicted in Fig. 1(b). The adsorption effects of glucose through different atoms on the WO₃ surface were examined under identical parametric conditions.

The optimization of transition-state structures utilized the climbing image nudged elastic band (CINEB)[41] and dimer methods[42], aiming to achieve force convergence within the criteria of 0.03 eV/Å. All identified transition states underwent further confirmation as first-order saddle points through finite difference normal-mode analysis, with only one imaginary frequency obtained at the transition state.

The adsorption energy (E_{ads}) was calculated by the following:

$$E_{ads} = E_{adsorbate+surface} - (E_{surface} + E_{adsorbate}) \quad (1)$$

Where $E_{adsorbate+surface}$ is the total energy of the adsorbate interacting with the surface slab, $E_{surface}$ is the total energy of the optimized surface slab, and $E_{adsorbate}$ is the energy of the intermediates in vacuum. Based on the above definition, a negative E_{ads} value indicates favorable (exothermic) adsorption.

The activation barriers (E_a) and reactions energies (ΔE) are defined as:

$$E_a = E_{TS} - E_{IS} \quad (2)$$

$$\Delta E = E_{FS} - E_{IS} \quad (3)$$

Where E_{IS}, E_{TS} and E_{FS} represent the total energies of initial states, transition states and final states, respectively. Negative value of ΔE refers to exothermic reaction.

III. RESULTS AND DISCUSSION

The mechanism of glucose conversion to glycolaldehyde is illustrated in Fig. 2, where glucose undergoes cleavage to form 1,2-ethenediol and erythrose. Subsequently, 1,2-ethenediol can be further transformed into glycolaldehyde through hydrogen atom migration, whereas erythrose breaks its C4-C5 bond to yield 1,2-ethenediol and glycolaldehyde. In this study, four adsorption configurations of glucose were primarily investigated to select the most optimal configuration as the starting point for calculations. This was followed by a thorough exploration of the reaction mechanism of glucose converting into glycolaldehyde on the WO₃(020) surface.
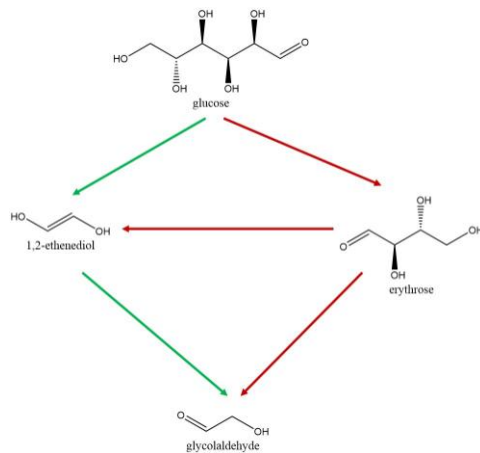
Fig. 2. The mechanism of glucose conversion to glycolaldehyde on WO₃(020) surface.

A. The four adsorption configurations of glucose molecules

As shown in Fig. 3, the optimization of the adsorption configurations of four glucose molecules on the WO₃ (020) surface was conducted, and the corresponding differential charge densities were calculated. The adsorption configuration parameters and energies of glucose on the WO₃(020) surface have been documented in Table 1.
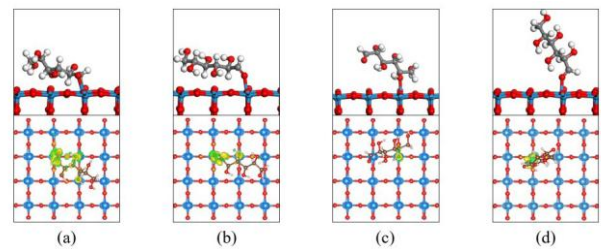
Fig. 3. The four adsorption configurations of glucosese molecules and differential charge density on WO₃(020) surface. (G1 (a), G2 (b), G3 (c), G4 (d))

Fig. 3(a) depicts glucose in G1 where C1, O1, O3, and O4 atoms are adsorbed above three W atoms on WO₃(020) surface. The C1-W bond length measures 2.178 Å, while the distances between O atoms (O1, O3, and O4) and the closest W atoms are 2.098 Å, 2.228 Å, and 2.340 Å respectively. The adsorption energy is calculated to be -3.06 eV. As illustrated in Fig. 3(b), glucose in G2 is adsorbed on the WO₃(020) surface through O1 and O3. The distances between O1, O3 atoms, and the nearest W atom are 1.969 Å and 2.281 Å respectively, with an adsorption energy of -2.57 eV. Fig. 3(c) demonstrates that glucose in G3 adsorbs on WO₃(020) surface through the O1 atom. The O1-W bond measures 2.025 Å in length with an adsorption energy of -1.52 eV. As shown in Fig. 3(d), glucose in G4 anchors via the O5 atom on WO₃(020), where the distance between the O5 atom and the surface is 2.229 Å, with an adsorption energy of -1.64 eV. The agreement between the results of differential charge density calculations and adsorption energy calculations indicates that in the G1 configuration, glucose exhibits the strongest interaction with the WO₃ surface and possesses a favorable geometric shape. Hence, it was selected as the starting point for the conversion process from glucose to glycolaldehyde..

TABLE 1: Aadsorption energies of glucose on wo₃(020) surface and configuration of glucose from this surface

Complexes	configuration	Adsorption site	Distance(Å)	E_{ads}(eV)
G1	C1–bound	W	2.178	-3.06
	O1–bound	W	2.098	
	O3–bound	W	2.288	
	O4–bound	W	2.340	
G2	O1–bound	W	1.969	-2.57
	O3–bound	W	2.281	
G3	O1–bound	W	2.025	-1.52
G4	O5–bound	W	2.229	-1.64

B. *The reaction mechanism involved in the cleavage of the C-C bond in glucose to form glycolaldehyde*

The elementary reactions involved in the cleavage of the cleavage of the C-C bond in glucose to form glycolaldehyde are illustrated in Fig. 4. Fig. 5 shows the potential energy surfaces involved in the conversion of glucose to glycolaldehyde on $WO_3(020)$ surface. The geometric parameters for initial states, transition states and final states of elementary reactions involved in the conversion of glucose to glycolaldehyde are listed in Table 2, with corresponding reaction barriers and reaction energies summarized in Table 3.
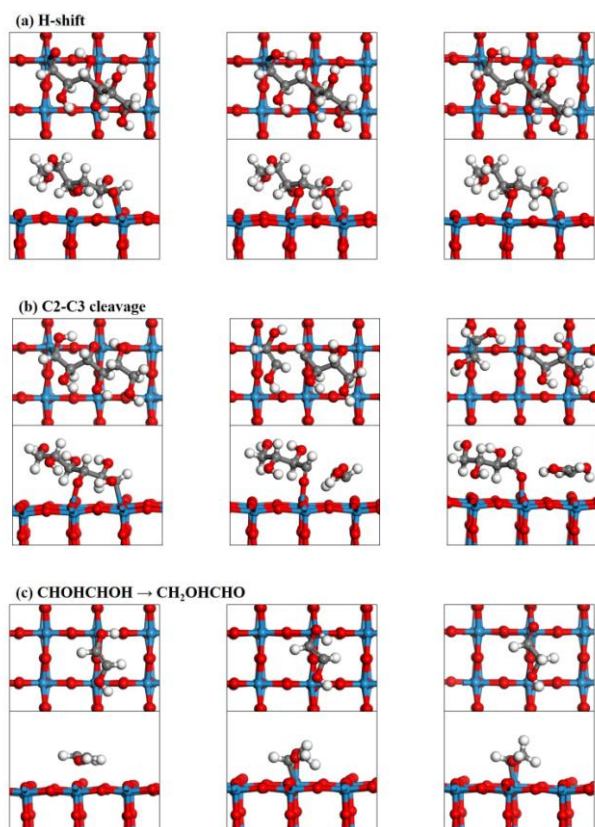

Fig. 4. Top and side views of initial states, transition states , and final states of elementary reactions involved in the cleavage of the C-C bond in glucose to form glycolaldehyde.
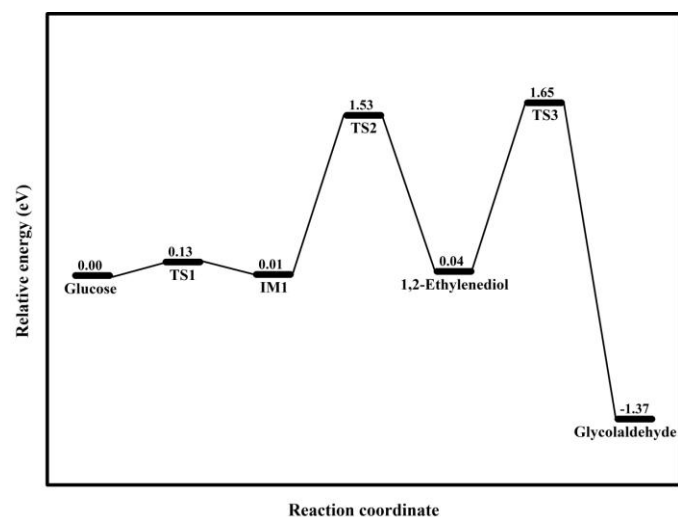

Fig. 5. The potential energy surfaces involved in the conversion of glucose to glycolaldehyde on $WO_3(020)$ surface.

Following glucose adsorption on the WO_3 surface, the transfer of the hydrogen atom (H3) from the hydroxyl group of C3 to the O atom on the aldehyde group. Geometrical parameters in Table 2 indicate bond lengths of 1.856 Å for O1–H3 and 1.007 Å for O3–H3 in the G1 structure. In the transition state (TS1), these values changed to 1.210 Å and 1.279 Å, respectively. The activation and reaction energies for this process were 0.13 eV and 0.30 eV, respectively, suggesting a straightforward H transfer. Subsequently, the cleavage of the C2–C3 bond in the product, formed by H transfer, led to the generation of 1,2-ethylenediol and erythrose. Bond lengths of C1–C2, C2–C3, and C3–O3 in IM1 were 1.528 Å, 1.563 Å, and 1.437 Å, respectively. Transitioning to the transition state (TS2), these lengths changed to 1.464 Å, 2.446 Å, and 1.318 Å, indicating C2–C3 cleavage and simultaneous formation of C1=C2 and C3=O double bonds. The activation energy and reaction energy for C2–C3 cleavage to produce 1,2-ethylenediol were 1.52 eV and 0.03 eV, respectively, signifying a slightly endothermic reaction. The H2 atom of the hydroxyl group of the C2 atom migrates to the C1 atom, forming glycolaldehyde. The calculated structure of 1,2-ethenediol displays bond lengths of 2.493 Å and 0.984 Å for C1–H2 and O2–H2, respectively. In the transition state, these values change to 1.263 Å and 1.567 Å, respectively, with activation and reaction energies of 1.61 eV and -1.41 eV, respectively. The elementary reaction of converting 1,2-ethylenediol to glycolaldehyde, involving the breaking of the C2-C3 bond in glucose to form glycolaldehyde, requires overcoming the highest energy barrier. This could be attributed to the relatively stable hydroxyl group in 1,2-ethylenediol, making the O-H bond less prone to breaking.

TABLE 2: THE GEOMETRIC PARAMETERS (Å) FOR INITIAL STATES (IS), TRANSITION STATES (TS), AND FINAL STATES (FS) OF ELEMENTARY REACTIONS INVOLVED IN THE CONVERSION OF GLUCOSE TO GLYCOLALDEHYDE.

Elementary reaction	Parameter	IS	TS	FS
H–shift	O1–H3	1.856	1.210	1.006
	O3–H3	1.007	1.279	1.873
C2–C3 cleavage	C1–C2	1.528	1.464	1.378
	C2–C3	1.563	2.446	4.623
	C3–O3	1.437	1.318	1.300
CHOHCHOH→ CH₂OHCHO	O1–H3	0.984	1.263	2.029
	C2-H3	2.493	1.567	1.105
H-shift	O5-H5	1.004	1.378	2.102
	O3-H5	1.829	1.118	0.986
C4-C5 cleavage	C3-C4	1.538	1.447	1.370
	C4-C5	1.560	2.473	4.418
	C5-O5	1.422	1.335	1.285

TABLE 3: THE REACTION BARRIERS AND REACTION ENERGIES (ΔE) OF ELEMENTARY REACTIONS INVOLVED IN THE CONVERSION OF GLUCOSE TO GLYCOLALDEHYDE.

Elementary reaction	Reaction barrier(eV)	Reaction energy(eV)
H-shift	0.13	0.01

C2–C3 cleavage	1.52	0.03
CHOHCHOH→CH$_2$OHCHO	1.61	-1.41
H-shift	0.17	0.04
C4-C5 cleavage	1.02	0.55

C. The reaction mechanism involved in the cleavage of the C-C bond in erythrose to form glycolaldehyde

Erythrose, a C4 product resulting from the cleavage of the C2-C3 bond in glucose, can also be further converted into erythrose via C-C bond cleavage. The optimized structures, including top and side views of the initial, transition, and final states of all elementary reactions involved in the cleavage of the C-C bond in erythrose to form glycolaldehyde on the WO$_3$(020) surface, are depicted in Fig. 6, with corresponding activation barriers and reaction energies summarized in Fig. 7. Comprehensive details regarding the initial states, transition states, and final states involved in erythrose to form glycolaldehyde on the WO$_3$(020) surface are presented in Table 2. Further insights into activation barriers and reaction energies for these steps are succinctly summarized in Table 3
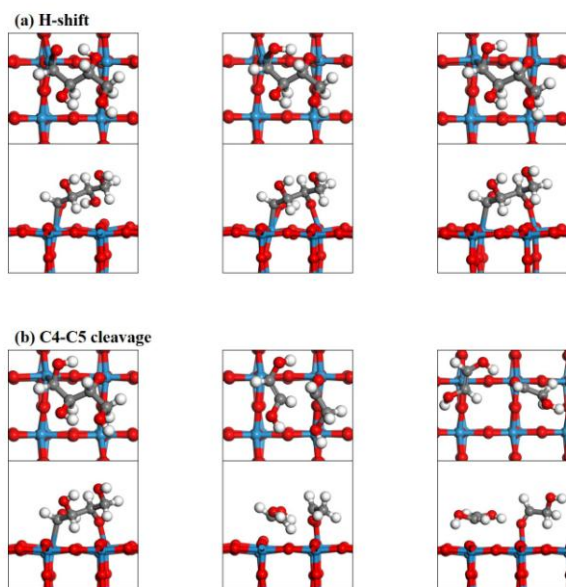

Fig. 6. Top and side views of initial states, transition states , and final states of elementary reactions involved in the cleavage of erythrose to form glycolaldehyde.

Similar to glucose, erythrose undergoes an initial H-atom transfer reaction where the H5 atom transitions from the O5 atom to the O3 atom, resulting in the formation of intermediate product IM2. Calculations reveal that the O5–H5 bond length erythrose is 1.004 Å, stretching to 1.378 Å at the transition state (TS4). The activation energy barrier for this process is determined to be 0.17 eV, with a reaction energy of 0.04 eV. Subsequently, the cleavage of the C–C bond in IM2 led to the generation of glycolaldehyde and 1,2-ethylenediol. Bond lengths of C3–C4, C4–C5, and C5–O5 in IM2 were 1.538 Å, 1.560 Å, and 1.422 Å, respectively. Transitioning to the transition state (TS5), these lengths changed to 1.447 Å, 2.473 Å, and 1.335 Å, indicating C4–C5 cleavage and simultaneous formation of C3=C4 and C5=O double bonds. The reaction barrier and reaction energy for C4–C5 cleavage to produce glycolaldehyde and 1,2-ethylenediol were 1.02 eV and 0.55 eV, respectively. The cleavage of the C4-C5 bond in erythrose leads to the formation of 1,2-ethylenediol, which can be further transformed into erythrose through an H-atom transfer. In
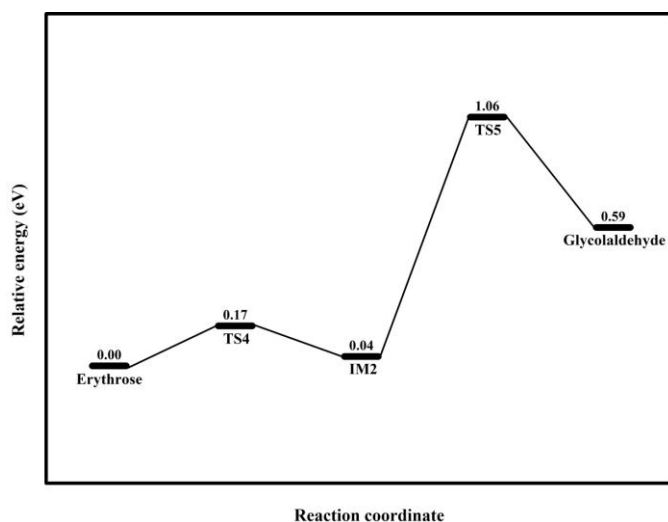
comparison, the energy barrier for the conversion of 1,2-ethylenediol generated from glucose cleavage into erythrose is higher than that for the further cleavage of erythrose produced from glucose cleavage into erythrose（1.61 eV VS 1.02 eV）.

Fig. 7. The potential energy surfaces involved in the conversion of erythrose to glycolaldehyde on WO$_3$(020) surface.

CONCLUSION

This study investigates the adsorption of glucose on the WO$_3$ surface and the reaction mechanism of the catalytic conversion of glucose to glycolaldehyde on WO$_3$(020) surface. The glucose conformation adsorbed on the surface, involving four atoms (C1, O1, O3, and O4), exhibits optimal geometry with the lowest adsorption energy (-3.06 eV). This conformation serves as the starting point for the catalytic conversion of glucose to glycolaldehyde. Comparing the two pathways for catalytic conversion of glucose to glycolaldehyde on WO$_3$(020) surface, The reaction barrier for the conversion of 1,2-ethylenediol produced from glucose degradation to glycolaldehyde is 1.61 eV, whereas the reaction barrier for the conversion of erythrose resulting from glucose degradation to glycolaldehyde is 1.02 eV. Therefore, in this investigation, the pathway involving glucose degradation to erythrose, followed by its subsequent breakdown to form glycolaldehyde, is considered the faster route for glucose conversion to glycolaldehyde.

References

[1] G.W. Huber, S. Iborra, A. Corma, Synthesis of Transportation Fuels from Biomass: Chemistry, Catalysts, and Engineering, Chemical Reviews, 106 (2006) 4044-4098.
[2] A. Corma, S. Iborra, A. Velty, Chemical Routes for the Transformation of Biomass into Chemicals, Chemical Reviews, 107 (2007) 2411-2502.
[3] R. Rinaldi, F. Schüth, Design of solid catalysts for the conversion of biomass, Energy & Environmental Science, 2 (2009) 610-626.
[4] W. Marquardt, A. Harwardt, M. Hechinger, K. Kraemer, J. Viell, A. Voll, The biorenewables opportunity - toward next generation process and product systems, AIChE Journal, 56 (2010) 2228-2235.
[5] C.-H. Zhou, X. Xia, C.-X. Lin, D.-S. Tong, J. Beltramini, Catalytic conversion of lignocellulosic biomass to fine chemicals and fuels, Chemical Society Reviews, 40 (2011) 5588-5617.
[6] H. Kobayashi, T. Komanoya, S.K. Guha, K. Hara, A. Fukuoka, Conversion of cellulose to renewable chemicals by supported metal catalysis, Applied Catalysis A: General, 409-410 (2011) 13-20.
[7] P. Gallezot, Conversion of biomass to selected chemical products, Chemical Society Reviews, 41 (2012) 1538-1558.

[8] Y. Wang, W. Deng, B. Wang, Q. Zhang, X. Wan, Z. Tang, Y. Wang, C. Zhu, Z. Cao, G. Wang, H. Wan, Chemical synthesis of lactic acid from cellulose catalysed by lead(II) ions in water, Nature Communications, 4 (2013) 2141.

[9] G. Li, N. Li, S. Li, A. Wang, Y. Cong, X. Wang, T. Zhang, Synthesis of renewable diesel with hydroxyacetone and 2-methyl-furan, Chemical Communications, 49 (2013) 5727-5729.

[10] P. Daoutidis, W.A. Marvin, S. Rangarajan, A.I. Torres, Engineering Biomass Conversion Processes: A Systems Perspective, AIChE Journal, 59 (2013) 3-18.

[11] Y. Wang, F. Jin, M. Sasaki, Wahyudiono, F. Wang, Z. Jing, M. Goto, Selective conversion of glucose into lactic acid and acetic acid with copper oxide under hydrothermal conditions, AIChE Journal, 59 (2013) 2096-2104.

[12] B. Joffres, C. Lorentz, M. Vidalie, D. Laurenti, A.A. Quoineaud, N. Charon, A. Daudin, A. Quignard, C. Geantet, Catalytic hydroconversion of a wheat straw soda lignin: Characterization of the products and the lignin residue, Applied Catalysis B: Environmental, 145 (2014) 167-176.

[13] T. Yoshikawa, S. Shinohara, T. Yagi, N. Ryumon, Y. Nakasaka, T. Tago, T. Masuda, Production of phenols from lignin-derived slurry liquid using iron oxide catalyst, Applied Catalysis B: Environmental, 146 (2014) 289-297.

[14] M. Li, G. Li, N. Li, A. Wang, W. Dong, X. Wang, Y. Cong, Aqueous phase hydrogenation of levulinic acid to 1,4-pentanediol, Chemical Communications, 50 (2014) 1414-1416.

[15] D.M. Alonso, J.Q. Bond, J.A. Dumesic, Catalytic conversion of biomass to biofuels, Green Chemistry, 12 (2010) 1493-1513.

[16] K. Hirajima, M. Taguchi, T. Funazukuri, Semibatch Hydrothermal Hydrolysis of Cellulose in a Filter Paper by Dilute Organic Acids, Industrial & Engineering Chemistry Research, 54 (2015) 6052-6059.

[17] M.E. Himmel, S.-Y. Ding, D.K. Johnson, W.S. Adney, M.R. Nimlos, J.W. Brady, T.D. Foust, Biomass Recalcitrance: Engineering Plants and Enzymes for Biofuels Production, Science, 315 (2007) 804-807.

[18] N. Wei, J. Quarterman, S.R. Kim, J.H.D. Cate, Y.-S. Jin, Enhanced biofuel production through coupled acetic acid and xylose consumption by engineered yeast, Nature Communications, 4 (2013) 2580.

[19] L. Bui, H. Luo, W.R. Gunther, Y. Román-Leshkov, Domino Reaction Catalyzed by Zeolites with Brønsted and Lewis Acid Sites for the Production of γ-Valerolactone from Furfural, Angewandte Chemie International Edition, 52 (2013) 8022-8025.

[20] M. Shiramizu, F.D. Toste, Expanding the Scope of Biomass-Derived Chemicals through Tandem Reactions Based on Oxorhenium-Catalyzed Deoxydehydration, Angewandte Chemie International Edition, 52 (2013) 12905-12909.

[21] N. Villandier, A. Corma, One pot catalytic conversion of cellulose into biodegradable surfactants, Chemical Communications, 46 (2010) 4408-4410.

[22] H. Danner, R. Braun, Biotechnology for the production of commodity chemicals from biomass, Chemical Society Reviews, 28 (1999) 395-405.

[23] J.J. Wiesfeld, P. Peršolja, F.A. Rollier, A.M. Elemans-Mehring, E.J.M. Hensen, Cellulose conversion to ethylene glycol by tungsten oxide-based catalysts, Molecular Catalysis, 473 (2019) 110400.

[24] L.S. Ribeiro, N. Rey-Raap, J.L. Figueiredo, J.J. Melo Órfão, M.F.R. Pereira, Glucose-based carbon materials as supports for the efficient catalytic transformation of cellulose directly to ethylene glycol, Cellulose, 26 (2019) 7337-7353.

[25] H. Xin, H. Wang, S. Li, X. Hu, C. Wang, L. Ma, Q. Liu, Efficient production of ethylene glycol from cellulose over Co@C catalysts

[26] combined with tungstic acid, Sustainable Energy & Fuels, 6 (2022) 2602-2612.

[26] Q. Liu, H. Wang, H. Xin, C. Wang, L. Yan, Y. Wang, Q. Zhang, X. Zhang, Y. Xu, G.W. Huber, L. Ma, Selective Cellulose Hydrogenolysis to Ethanol Using Ni@C Combined with Phosphoric Acid Catalysts, ChemSusChem, 12 (2019) 3977-3987.

[27] M. Yang, H. Qi, F. Liu, Y. Ren, X. Pan, L. Zhang, X. Liu, H. Wang, J. Pang, M. Zheng, A. Wang, T. Zhang, One-Pot Production of Cellulosic Ethanol via Tandem Catalysis over a Multifunctional Mo/Pt/WOx Catalyst, Joule, 3 (2019) 1937-1948.

[28] C. Li, G. Xu, C. Wang, L. Ma, Y. Qiao, Y. Zhang, Y. Fu, One-pot chemocatalytic transformation of cellulose to ethanol over Ru-WOx/HZSM-5, Green Chemistry, 21 (2019) 2234-2239.

[29] Y. Zhang, J. Cao, Y. Zhou, Y. Li, L. Li, X.-a. Xie, MoO3–catalyzed transformation of corn stalk cellulose to glycolic acid: an experimental and DFT study, Cellulose, 30 (2023) 3523-3537.

[30] V.R. Madduluri, M.Y. Lim, A.S. Saud, G.P. Maniam, M.H. Ab Rahim, Direct Valorization of Cellulose and Glucose to Glycolic Acid through Green Catalytic Process, Catalysis Letters, 154 (2024) 994-1006.

[31] F. Wang, W. Dong, D. Qu, Y. Huang, Y. Chen, Synergistic Catalytic Conversion of Cellulose into Glycolic Acid over Mn-Doped Bismuth Oxyiodide Catalyst Combined with H-ZSM-5, Industrial & Engineering Chemistry Research, 61 (2022) 11382-11389.

[32] A. Wang, T. Zhang, One-Pot Conversion of Cellulose to Ethylene Glycol with Multifunctional Tungsten-Based Catalysts, Accounts of Chemical Research, 46 (2013) 1377-1386.

[33] J. Zhang, B. Hou, A. Wang, Z. Li, H. Wang, T. Zhang, Kinetic study of retro-aldol condensation of glucose to glycolaldehyde with ammonium metatungstate as the catalyst, AIChE Journal, 60 (2014) 3804-3813.

[34] J. Zhang, B. Hou, A. Wang, Z. Li, H. Wang, T. Zhang, Kinetic study of the competitive hydrogenation of glycolaldehyde and glucose on Ru/C with or without AMT, AIChE Journal, 61 (2015) 224-238.

[35] G. Zhao, M. Zheng, J. Zhang, A. Wang, T. Zhang, Catalytic Conversion of Concentrated Glucose to Ethylene Glycol with Semicontinuous Reaction System, Industrial & Engineering Chemistry Research, 52 (2013) 9566-9572.

[36] Y. Liu, C. Luo, H. Liu, Tungsten Trioxide Promoted Selective Conversion of Cellulose into Propylene Glycol and Ethylene Glycol on a Ruthenium Catalyst, Angewandte Chemie International Edition, 51 (2012) 3249-3253.

[37] Kresse, Furthmuller, Efficient iterative schemes for ab initio total-energy calculations using a plane-wave basis set, Physical review. B, Condensed matter, 54 (1996) 11169-11186.

[38] G. Kresse, J. Furthmüller, Efficiency of ab-initio total energy calculations for metals and semiconductors using a plane-wave basis set, Computational Materials Science, 6 (1996) 15-50.

[39] M. Ernzerhof, G.E.J.J.o.C.P. Scuseria, Assessment of the Perdew–Burke–Ernzerhof exchange-correlation functional, 110 (1999) 5029-5036.

[40] J.P. Perdew, K. Burke, M. Ernzerhof, Generalized Gradient Approximation Made Simple, Physical Review Letters, 77 (1996) 3865-3868.

[41] G.A. Henkelman, B.P. Uberuaga, H.J.J.o.C.P. Jónsson, A climbing image nudged elastic band method for finding saddle points and minimum energy paths, 113 (2000) 9901-9904.

[42] G. Henkelman, H. Jónsson, A dimer method for finding saddle points on high dimensional potential surfaces using only first derivatives, The Journal of Chemical Physics, 111 (1999) 7010-7022.